March - April 2020
ISSN: 0193-4120 Page No. 16980 - 16989

Physical-based Nano Indentation Simulation of Single Crystals

[1]Sina Soleimani, [2]Asghar Zajkani *
[1,2]Department of Mechanical Engineering, Imam Khomeini International University, Qazvin, Iran
* Email: zajkani@eng.ikiu.ac.ir
Postal code: 3414896818

Article Info
Volume 83
Page Number: 16980 - 16989
Publication Issue:
March - April 2020

Article History
Article Received*: 24 July 2019*
Revised*: 12 September 2019*
Accepted*: 15 February 2020*
Publication*: 28 April 2020*

Abstract
In this article, a loading process of the micro/Nano-indentation test is simulated based on physical plasticity. The total energy of process is obtained by evaluating different terms such as dislocations density energy, energy caused by contact of indenter to the material and other terms of classic mechanic's. The physical domain of region beneath the indenter is mapped to a unit cubic domain as a computational domain by using a homographic mapping formulation. For the first time by using the principle of minimum energy differential equations of the micro-indentation process is evaluated for a FCC crystal. Three main coupled differential equations, twelve necessary robin boundary conditions and eight physical boundary conditions are solved by using a generalized differential quadrature method based on the Gauss-Chebyshev-Lobato polynomials. It is seen that the applied method is more efficient and gets closer results to experiments. Finally, material behavior to different conical angles of indenter for the FCC crystal is compared.
Keywords: *Micro/Nano indentation, Homographic mapping, Minimum energy, FCC crystal.*

I. INTRODUCTION

Indentation test is used for determining materials characteristics at different depths, involving a striking size effect. It was seen that by decreasing indentation depth, measured hardness increases. Unlike the common believe between researchers, the hardness is not a characteristic of the small size [1]. Taylor represented that crystal defect has a great role in plastic deformations mechanisms by presenting an analytical model [2]. This size effect is because of dislocations nucleation, where resolved shear stress on slip planes of crystals reaching a critical threshold. These types of dislocations are called the geometrically necessary dislocations (GND), which are necessary to form crystal due to the certain loading. Many researchers did investigations to present better models and simulations for dislocations interactions and dislocations movements by developing some fundamental concepts such as dislocations density, dislocations generation, and classification of dislocation types [3]–[6] and [7]. The crystal plasticity theories explain crystalline material behavior to applied load by utilizing dislocations density concepts.

Berdichevsky analyzed the problem with an energy-based view. [8]–[14]. Berdichevsky proposed a saturated density function which could be evaluated by using geometrically

March - April 2020
ISSN: 0193-4120 Page No. 16980 - 16989

necessary and statistically stored dislocation densities. He derived energy function that is caused by dislocations densities by using the saturated density function[8]. Moreover, during past few years, a new approach has been proposed based on continuum dislocation dynamics [15]–[18]. The approach could predict both dislocation densities and curvature and direction of dislocation lines. The high computational cost in problems like indentation has been one of the reasons to not to use this method. Baitsch et al. analyzed two- dimensional plane-strain problem of wedge indentation for a single crystal having only one active slip system on each side of the wedge by using finite element method to discretize governing equation and applying a Newton-Raphson procedure to obtain minimizer numerically [19].

The material proposed in this paper is based on continuum dislocation theory developed in following references [12]–[14] and [20]–[22]. In the present article, the micro-indentation of a wedge indenter into an FCC single crystal is analyzed. The governing equations of the process are evaluated by utilizing minimum energy principle. Three coupled differential equations besides twelve necessary boundary conditions and seven physical boundary conditions are discretized by using generalized differential quadrature method. Load-displacement loading curve and three field variables (transverse displacement field, longitudinal displacement field, and plastic distortion field) on nodal points of the physical domain are evaluated. It is seen that proposed method has more accurate results than previous models.

II. PRIMARY KINEMATICS

According to Fig. 1 consider a rigid wedge indenter that gets into a single crystal. Size of the single crystal is considered significant enough to be sure the plane strain state having two component of displacements $u(x,y), v(x,y)$. According to the wedge shape of the indenter and the axial symmetry conditions, a half section of material beneath the indenter is analyzed. It is assumed that just one slip system is active where $s = (cos\emptyset, sin\emptyset)^T$ expresses the slip direction and $m = (-sin\emptyset, cos\emptyset)^T$ denotes the normal vector to slip plane. The plastic distortion field is defined as $\beta = \beta(x,y)\boldsymbol{s}\otimes\boldsymbol{m}$. According to physics of problem and assumptions made about material properties, all tensors and field variables are considered two-dimensional. Regarding the longitudinal displacement of the indenter is – h, which is the control parameter of the problem as input. Loading process would be captured by evaluating displacement fields $u(x,y), v(x,y)$, and the plastic distortion $\beta(x,y)$ for steps of loading.

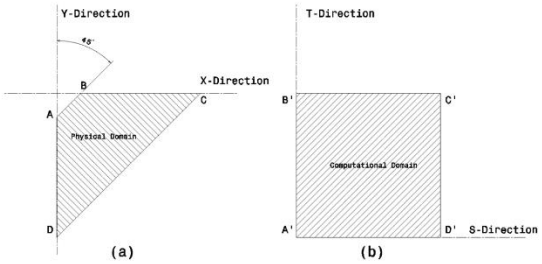

Figure 1: (a) Physical domain of material beneath the indenter. (b) Computational domain after applying homographic mapping

March - April 2020
ISSN: 0193-4120 Page No. 16980 - 16989

For a plane- strain state, the in-plane components of the symmetric strain tensor can be evaluated by the following relations:

$$\varepsilon_{xx} = u_{,x}$$

$$\varepsilon_{xy} = \frac{1}{2}(u_{,y} + v_{,x}) \quad (1)$$

$$\varepsilon_{yy} = v_{,y}$$

The in-plane components of the symmetric plastic strain tensor would be evaluated as:

$$\varepsilon^p_{xx} = -\frac{1}{2}\beta sin2\emptyset$$

$$\varepsilon^p_{xy} = \frac{1}{2}\beta cos2\emptyset \quad (2)$$

$$\varepsilon^p_{yy} = \frac{1}{2}\beta sin2\emptyset$$

According to two above equations the elastic strain can be obtained by relation $\varepsilon^e = \varepsilon - \varepsilon^p$ as:

$$\varepsilon^e_{xx} = u_{,x} + \frac{1}{2}\beta \sin 2\emptyset$$

$$\varepsilon^e_{xy} = \frac{1}{2}(u_{,y} + v_{,x} - \beta \cos 2\emptyset) \quad (3)$$

$$\varepsilon^e_{yy} = v_{,y} - \frac{1}{2}\beta \sin 2\emptyset$$

Regarding Nye-Bilby-Kroner's dislocation density tensor: $\alpha = -\beta \times \nabla$, that $\times$ is vector product ([23] and [24]), for plane strain plastic distortion, just two nonzero components remain as:

$$\alpha_{xz} = (\beta_{,x} \cos\emptyset + \beta_{,y} \sin\emptyset) \sin\emptyset \quad (4)$$

$$\alpha_{yz} = (\beta_x \cos\emptyset + \beta_{,y} \sin\emptyset) \sin\emptyset$$

Two above equations are net Burger's vector components of all excess dislocations that dislocation lines cut the unit area perpendicular to the z-axis. It is seen that just edge dislocations exist beneath the indenter because the net Burger's vector of excess dislocations is parallel to the slip direction s. The sign of $(\beta_{,x} \cos\emptyset + \beta_{,y} \sin\emptyset)$ represents that the excess dislocation being negative or positive. To know how many excess dislocations are generated per unit area that is called geometrically necessary dislocations density the length of net Burger's vector should be divided by the magnitude of Burger's vector, b.

$$\rho = \frac{1}{b}\sqrt{\alpha^2_{xz} + \alpha^2_{yz}} = \frac{1}{b}\left|\beta_{,x} \cos\emptyset + \beta_{,y} \sin\emptyset\right| \quad (5)$$

III. TOTAL ENERGY FUNCTIONAL

Most metals usually got small strain tensor ε^e. Thus, free energy per unit volume of the single crystal with continuously distributed dislocations can be evaluated in following form [8], [9]

$$\psi(\varepsilon^e, \rho) = \frac{1}{2}\lambda(tr\ \boldsymbol{\varepsilon}^e)^2 + \mu\ \boldsymbol{\varepsilon}^e : \boldsymbol{\varepsilon}^e + \mu k \ln\frac{1}{1 - \frac{\rho}{\rho_s}} \quad (6)$$

where λ and μ are Lame constants, ρ_s is the saturated dislocation density and k is the material constant. The first two terms represent elastic strain share of total energy, and the last term corresponds to the dislocation network share. The term $\left(\ln\frac{1}{1-\rho/\rho_s}\right)$ shows that energy network for small dislocation densities is the sum of non-interacting dislocations energy. The logarithmic term represents that increase in energy generated by dislocations for small values of dislocation densities is linear, and it gets infinity when dislocation density gets closer to the saturated dislocation density. This point provides an energetic barrier against over-saturation. From the above equations the energy density per unit volume

March - April 2020
ISSN: 0193-4120 Page No. 16980 - 16989

of the crystal can be evaluated by the following equation:

$$\psi(\varepsilon^e,\rho)=\frac{1}{2}\lambda\left(u_{,x}+v_{,y}\right)^2+\mu\left(u_{,x}+\frac{1}{2}\beta\sin 2\emptyset\right)^2+\mu\left(u_{,x}-\frac{1}{2}\beta\sin 2\emptyset\right)^2+\frac{1}{2}\mu\left(u_{,y}+v_{,x}-\beta\cos 2\emptyset\right)^2+\mu k\ln\frac{1}{1-\frac{\rho}{\rho_s}}$$

If due to axisymmetric of the domain, Ω is the half plane of the occupied physical domain of deformed crystal beneath the indenter, the elastic energy and dislocations generation energy functional per unit depth can be formulated as:

$$I[u,v,\beta]=\int_\Omega\left[\frac{1}{2}\lambda\left(u_{,x}+v_{,y}\right)^2+\mu\left(u_{,x}+\frac{1}{2}\beta\sin 2\emptyset\right)^2+\mu\left(u_{,x}-\frac{1}{2}\beta\sin 2\emptyset\right)^2+\frac{1}{2}\mu\left(u_{,y}+v_{,x}-\beta\cos 2\emptyset\right)^2+\mu k\ln\frac{1}{1-\frac{\rho}{\rho_s}}\right]dxdy$$

Variation of contact energy can be evaluated as [25]:

$$\delta\Pi^c=\int_{\Gamma_c}(\lambda_N\cdot\delta g_N+t_T\cdot\delta g_T)dA+\int_{\Gamma_c}\delta\lambda_N\cdot g_N dA$$

where λ_N, is Lagrange Multiplier which represents normal contact force over the contact surface. The parameters g_N, t_T, and dA are normal gap function, tangential gap function, and surface element, respectively.By assuming w^1, w^2 and n^1 as deformation of first body(material beneath the indenter), the second body(indenter) and a normal vector to the contact surface, the normal gap function are obtained by the following equation:

$$g_N=\left(w^2_{(u,v)}-w^1_{(u,v)}\right)\cdot n^1 \quad (10)$$

For a wedge indenter with a cone angle of θ the normal vector would be evaluated as:

$$n^1=\sin\frac{\theta}{2}\boldsymbol{i}+\cos\frac{\theta}{2}\boldsymbol{j} \quad (11)$$

By assuming penetration of rigid indenter variation of contact energy functional would be obtained as:

$$\delta\Pi^c=\int_{\Gamma_c}\left[\lambda_N\cos\frac{\theta}{2}\delta u-\lambda_N\sin\frac{\theta}{2}\delta v+\left(\cos\frac{\theta}{2}u-\sin\frac{\theta}{2}v\right)\delta\lambda_N\right]dA_c$$

The total energy functional would be obtained from the above equation:

$$\delta\Pi^{total}=\delta\Pi^c+\delta I \quad (13)$$

IV. MAPPING AND EQUATIONS

By using a Homographic mapping, any quadrilateral shape can be mapped into another quadrilateral, as shown in Fig.1. The mapping can be done by using two following relations:

$$X=\frac{ax+by+c}{gx+hy+1},\qquad Y=\frac{dx+ey+f}{gx+hy+1} \quad (14)$$

where a,b,c,d,e,f,g and h are homographic mapping constants. By solving following system of equations, mapping constants can be evaluated.

$$\begin{bmatrix}x_1&y_1&1&0&0&0&-x_1X_1&-y_1Y_1\\x_2&y_2&1&0&0&0&-x_2X_2&-y_2Y_2\\x_3&y_3&1&0&0&0&-x_3X_3&-y_3Y_3\\x_4&y_4&1&0&0&0&-x_4X_4&-y_4Y_4\\0&0&0&x_1&y_1&1&-x_1Y_1&-y_1X_1\\0&0&0&x_2&y_2&1&-x_2Y_2&-y_2X_2\\0&0&0&x_3&y_3&1&-x_3Y_3&-y_3X_3\\0&0&0&x_4&y_4&1&-x_4Y_4&-y_4X_4\end{bmatrix}\cdot\begin{bmatrix}a\\b\\c\\d\\e\\f\\g\\h\end{bmatrix}=\begin{bmatrix}X_1\\X_2\\X_3\\X_4\\Y_1\\Y_2\\Y_3\\Y_4\end{bmatrix} \quad (15)$$

where x_i, y_i, X_i, and Y_i for $i=1,2,3,4$ are quadrilateral corners of physical domain and computational domain.

To avoid appearing too much zero arrays in the above matrix, before using homographic mapping the domain is translated one

March - April 2020
ISSN: 0193-4120 Page No. 16980 - 16989

micrometer along x-direction and y-direction. By implementing translation and homographic mapping and rewriting total energy functional and applying variation operator, the governing equations and the fundamental equation will be evaluated as below. Due to axisymmetric of physical domain over y-direction horizontal displacement and plastic distortion fields are zero. It is assumed that stick occurs over contact region (AB edge), by implementing this assumption the horizontal displacement and plastic distortion variables would be zero over this boundary too. It is assumed that no vertical displacement occurs over BC edge.

V. PHYSICAL BOUNDARY CONDITIONS

Derived equation caused by δu:

$$A_1\, v_{,t} + A_2\, v_{,tt} + A_3\, v_{,ts} + A_4\, v_{,s} + A_5\, v_{,ss} + A_6\, u_{,t} + A_7\, u_{,s} + A_8\, u_{,tt} + A_9\, u_{,ss} + A_{10}\, u_{,ts} + A_{11}\, \beta + A_{12}\, \beta_t + A_{13}\, \beta_{,s} = A_{Constant} \quad (1$$

Derived equation caused by δv:

$$B_1\, v_{,t} + B_2\, v_{,tt} + B_3\, v_{,ts} + B_4\, v_{,s} + B_5\, v_{,ss} + B_6\, u_{,t} + B_7\, u_{,s} + B_8\, u_{,tt} + B_9\, u_{,ss} + B_{10}\, u_{,ts} + B_{11}\, \beta + B_{12}\, \beta_t + B_{13}\, \beta_{,s} = B_{Constant} \quad (1$$

Derived equation caused by $\delta\beta$:

$$C_1\, v_{,t} + C_2\, v_{,s} + C_3\, u_{,t} + C_4 u_{,s} + C_5\, \beta + C_6\, \beta_{,t} + C_7\, \beta_{,s} + C_8\, \frac{\partial^2 \beta}{\partial t^2} + C_9\, \beta_{,ss} + C_{10}\, \beta_{,st} = C_{Constant} \quad (1$$

In above equations, A_n, B_n, C_m for $m = 1 \dots 11$ and $n = 1 \dots 13$ are differential equation terms coefficients which vary all over the computational domain. Derived equation caused by $\delta\lambda_N$ contact energy over $t = 1$ boundary:

$$M_1 u + N_1 v = 0 \quad (19)$$

The parameters M_1 and N_1 are coefficients of terms caused by contact energy which vary along contact Boundary.

By using Euler-Lagrange equation twelve necessary boundary conditions would be evaluated over four boundaries of domain, caused by three independent field variables. By enforcing physical boundary conditions only four essential boundary condition equations remain which are as following equations:

$$BC1_1 v_{,t} + BC1_2 v_{,s} + BC1_3 \beta + BC1_4 u_{,t} + BC1_5 u_{,s} = BC1_{Constant} \quad (2$$

$$BC2_1 v_{,t} + BC2_2 v_{,s} + BC2_3 \beta + BC2_4 u_{,t} + BC2_5 u_{,s} = BC2_{Constant} \quad (2$$

$$BC3_1 \beta_t + BC3_2 \beta_s = BC3_{Constant} \quad (2$$

$$BC4_1 \beta_t + BC4_2 \beta_s = BC4_{Constant} \quad (2$$

$BC1_i$, $BC2_i$, $BC3_j$, $BC4_j$ for $i = 1 \dots 4$, $j = 1 \dots 2$ $BC1_{Constant}$, $BC2_{Constant}$, $BC3_{Constant}$ and $BC4_{constant}$ are Robin boundary conditions terms coefficients and constants which are dependent to the point that analysis is done.

VI. GENERALIZED DIFFERENTIAL QUADRATURE METHOD

Generalized differential quadrature is a mathematical method to discretized differential equations and computational domain. The s and t are directions, where the computational domain is discretized to N_s and N_s part. A Chebyshev-Gauss-Lobato function is used to distribute points over the domain as following formulas:

$$s_i = \frac{1-\cos\frac{i-1}{N_s-1}\pi}{2}, \qquad i = 1..N_s$$
$$t_j = \frac{1-\cos\frac{j-1}{N_t-1}\pi}{2}, \qquad i = 1..N_s \tag{24}$$

The n-th order of derivative of $f(s,t)$ with respect to s and the m-th order derivative of $f(s,t)$ with respect to t can be discretized at s_i , t_i as [26]:

$$f_s^{(n)}(s_i,t_j) = \sum_{k=1}^{N_s} W_{ik}^{(n)} f(s_k,t_j)\,; \quad n = 1..N_s, \quad i = 1..N_s, \quad j = 1..N_t$$

and

$$f_t^{(m)}(s_i,t_j) = \sum_{k=1}^{N_t} \bar{W}_{ik}^{(m)} f(s_k,t_j), \quad m = 1..N_t\ ,\ i = 1..N_s\ ,\ j = 1..N_t \tag{26}$$

where $W_{ik}^{(n)}$ and $\bar{W}_{ik}^{(m)}$ are weighting coefficients. Non-diagonal arrays of weighting coefficients can be evaluated along s and t direction respectively, as:

$$W_{ij}^{(n)} = \frac{\prod_{j=1,j\neq i}^{N_s}(s_i - s_j)}{(s_i - s_j)\prod_{i=1,i\neq j}^{N_s}(s_j - s_i)}$$
$$\bar{W}_{ij}^{(n)} = \frac{\prod_{j=1,j\neq i}^{N_t}(t_i - t_j)}{(t_i - t_j)\prod_{i=1,i\neq j}^{N_t}(t_j - t_i)} \tag{27}$$

Moreover, the diagonal arrays of weighting coefficients along s and t directions can be evaluated, respectively as:

$$W_{ii}^{(1)} = -\prod_{i=1,i\neq j}^{N_s} W_{ji}^{(1)} \tag{28}$$

$$\bar{W}_{ii}^{(1)} = -\prod_{i=1,i\neq j}^{N_s} \bar{W}_{ji}^{(1)} \tag{29}$$

where t_i and s_i are the nodes coordinate in the computational domain. To evaluate the higher order derivatives of the diagonal and non-diagonal arrays; the following equation can be used:

$$W_{ik}^{(r)} = r\left[W_{ii}^{(r-1)} W_{ik}^{1} - \frac{W_{ik}^{(r-1)}}{s_i - s_k}\right] \tag{30}$$

$$W_{ii}^{(r)} = -\prod_{i=1,i\neq j}^{N_s} W_{ji}^{(r)} \tag{31}$$

$$\bar{W}_{ik}^{(r)} = r\left[\bar{W}_{ii}^{(r-1)} \bar{W}_{ik}^{1} - \frac{\bar{W}_{ik}^{(r-1)}}{t_i - t_k}\right] \tag{32}$$

$$\bar{W}_{ii}^{(r)} = -\prod_{i=1,i\neq j}^{N_t} \bar{W}_{ji}^{(r)} \tag{33}$$

where r is the order of derivatives. Discretization must be applied to the three governing equations and twelve necessary boundary conditions which are in differential form by using the Chebyshev-Gauss-Lobato point distribution over computational domain.

Unknown field variables such as horizontal and vertical displacement fields, plastic distortion field and the Lagrange multiplier, can be evaluated. Twelve steps loading of wedge indenter into a Ni single crystal is simulated. The Ni single crystal mechanical and crystallographic properties are presented in Table.1. Comparisons are made with the prior experimental and simulation researches with same indenter and material. The field variables are evaluated in the computational domain over a grid that is meshed by Chebyshev-Gauss-Lobato polynomials. To plot the contours of the field; the values of the field variables are mapped from computational domain to physical domain. The indenter is considered to remain rigid during the loading process.

March - April 2020
ISSN: 0193-4120 Page No. 16980 - 16989

Table.1 Mechanical and crystallographic properties of Ni single crystal

Properties	Symbol	Value	Unit
Lame' constant [27]	λ	116.63	GPa
Shear modulus	μ	94.66	GPa
Poisson coefficient [27]	υ	0.276	
Net Burgers vector [28]	b	2.5	Å
Material constant [19]	k	$4e+5$	
Saturated dislocations density [19]	ρ_s	$1e+5$	m^{-2}

As seen in Fig.2, the loading curve of the micro-indentation process of the rigid indenter into Ni single crystal for the present model is compared with experimental values [29] and previous model [19]. The vertical axis is indentation force over indentation depth values, and the horizontal axis is presenting indentation depth of indenter, as seen.

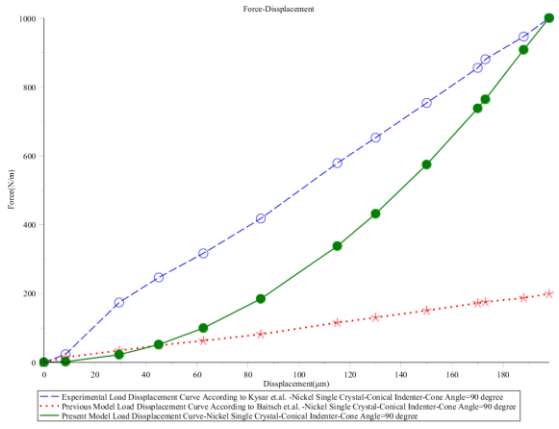

Figure 2 The comparison of the present model with the experimental values and the previous model

The reason of deviation of present results from experimental results is going to be discussed. One of the error sources is ignoring energy dissipation. Movements of dislocations and heat generation cause the energy dissipations due to slip occurrence. Previous researches have represented that in low strain rates, where loading process is semi-static the energy dissipation is ignorable [30]. In Fig.3, The indentation angles during micro indentation simulation in the present model is compared.

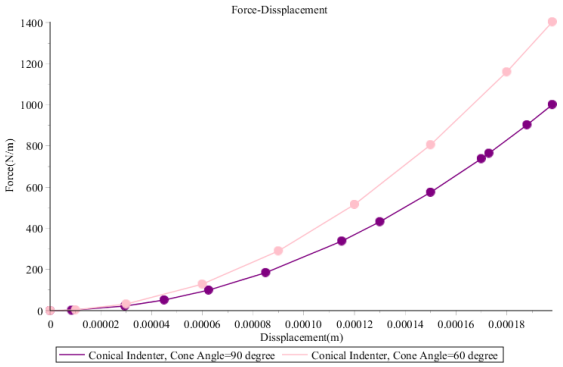

Figure 3 The comparison of the indentation angles during micro indentation simulation in the present model

In Fig.4, the plastic and elastic energies of Ni single crystalline material under micro indentation process for a 90degree conical indenter are plotted according to the indentation depth. It is seen that in 4th step of loading a sudden increase in plastic energy occurs, where elastic energy increases with a highest slope. It is seen that by penetrating indenter into material, elastic energy increases in all steps of loading, while plastic energy decreases

after 4th step. Elastic energy of indentation process is just related to displacement fields and increases by increasing indentation depth. On the other hand, plastic energy variation is caused by dislocation generation and annihilation which means, dislocation pile-ups and sink-ins. It is comprehended that in 4th step a dislocation plie-up occurs where plastic energy increases, where a dislocation sink-in occurs in 5th step of loading.

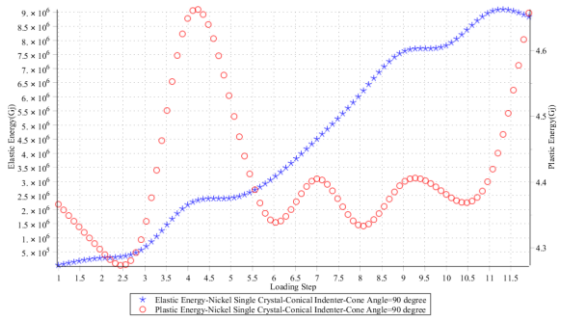

Figure 4 Plastic energy (red circles) and elastic energy (blue stars) according to indentation loading steps

CONCLUSION

By changing the angle of the indentation for the same loading, we obtained a different depth in the underlying material. By decreasing the angles of the deformation cone, an increase in the gradient of the displacement force was seen, indicating an increase in the elastic behavior of the material against sharper debris. The strengths of this research are to consider the effective parameters and not to ignore the effects that have a great impact on the solving method. it is seen that peak of plastic distortion field, dislocation density, plastic energy and strain are close to contact area. By taking a closer look at vertical and horizontal displacement fields and comparing with plastic distortion field it is seen that displacement fields are behaving like each other where it differs from plastic distortion field.

REFERENCES

[1] H. Gao, Y. Huang, W. D. Nix, and J. W. Hutchinson, “Mechanism-based strain gradient plasticity— I. Theory,” J. Mech. Phys. Solids, vol. 47, no. 6, pp. 1239–1263, 1999.

[2] G. I. Taylor, “The Mechanism of Plastic Deformation of Crystals. Part I. Theoretical,” Proc. R. Soc. A Math. Phys. Eng. Sci., vol. 145, no. 855, pp. 362–387, 1934.

[3] H. H. W. Physical, “I. Static theory,” vol. 198, pp. 205–216, 1949.

[4] W. G. Johnston and J. J. Gilman, “Dislocation Velocities, Dislocation Densities, and Plastic Flow in Lithium Fluoride Crystals,” J. Appl. Phys., vol. 30, no. 2, pp. 129–144, Feb. 1959.

[5] F. R. N. (Frank R. N. Nabarro, M. S. Duesbery, and J. P. Hirth, Dislocations in solids. North-Holland Pub. Co, 1979.

[6] A. Arsenlis and D. M. Parks, “Crystallographic aspects of geometrically-necessary and statistically-stored dislocation density,” Acta Mater., vol. 47, no. 5, pp. 1597–1611, 1999.

[7] D. Hull and D. J. Bacon, Introduction to dislocations. Butterworth-Heinemann, 2001.

[8] V. L. Berdichevsky, “Continuum theory of dislocations revisited,” Contin. Mech. Thermodyn., vol. 18, no. 3–4, pp. 195–222, Jul. 2006.

[9] V. L. Berdichevsky, “On thermodynamics of crystal plasticity,” Scr. Mater., vol. 54, no. 5, pp. 711–716, Mar. 2006.

[10] V. L. Berdichevsky and K. C. Le, “Dislocation nucleation and work hardening in anti-plane constrained shear,” Contin. Mech. Thermodyn., vol. 18, no. 7–8, pp. 455–467, Jan. 2007.

March - April 2020
ISSN: 0193-4120 Page No. 16980 - 16989

[11] M. Kaluza and K. C. Le, “On torsion of a single crystal rod,” Int. J. Plast., vol. 27, no. 3, pp. 460–469, Mar. 2011.

[12] D. M. Kochmann and K. C. Le, “Dislocation pile-ups in bicrystals within continuum dislocation theory,” Int. J. Plast., vol. 24, no. 11, pp. 2125–2147, Nov. 2008.

[13] D. M. Kochmann and K. C. Le, “Plastic Deformation of Bicrystals Within Continuum Dislocation Theory,” Math. Mech. Solids, vol. 14, no. 6, pp. 540–563, Aug. 2009.

[14] D. M. Kochmann and K. C. Le, “A continuum model for initiation and evolution of deformation twinning,” J. Mech. Phys. Solids, vol. 57, no. 6, pp. 987–1002, Jun. 2009.

[15] I. Groma, F. F. Csikor, and M. Zaiser, “Spatial correlations and higher-order gradient terms in a continuum description of dislocation dynamics,” Acta Mater., vol. 51, no. 5, pp. 1271–1281, Mar. 2003.

[16] A. Arsenlis, D. M. Parks, R. Becker, and V. V. Bulatov, “On the evolution of crystallographic dislocation density in non-homogeneously deforming crystals,” J. Mech. Phys. Solids, vol. 52, no. 6, pp. 1213–1246, Jun. 2004.

[17] S. Sandfeld, T. Hochrainer, M. Zaiser, and P. Gumbsch, “Continuum modeling of dislocation plasticity: Theory, numerical implementation, and validation by discrete dislocation simulations,” J. Mater. Res., vol. 26, no. 05, pp. 623–632, Mar. 2011.

[18] S. Sandfeld, T. Hochrainer, P. Gumbsch, and M. Zaiser, “Numerical implementation of a 3D continuum theory of dislocation dynamics and application to micro-bending,” Philos. Mag., vol. 90, no. 27–28, pp. 3697–3728, Sep. 2010.

[19] M. Baitsch, K. C. Le, and T. M. Tran, “Dislocation structure during microindentation,” Int. J. Eng. Sci., vol. 94, pp. 195–211, 2015.

[20] K. C. Le and P. Sembiring, “Plane constrained uniaxial extension of a single crystal strip,” Int. J. Plast., vol. 25, no. 10, pp. 1950–1969, Oct. 2009.

[21] K. C. Le and P. Sembiring, “Plane constrained shear of single crystal strip with two active slip systems,” J. Mech. Phys. Solids, vol. 56, no. 8, pp. 2541–2554, Aug. 2008.

[22] K. C. Le and P. Sembiring, “Analytical solution of plane constrained shear problem for single crystals within continuum dislocation theory,” Arch. Appl. Mech., vol. 78, no. 8, pp. 587–597, Aug. 2008.

[23] J. . Nye, “Some geometrical relations in dislocated crystals,” Acta Metall., vol. 1, no. 2, pp. 153–162, Mar. 1953.

[24] E. Kr�ner, “Der fundamentale Zusammenhang zwischen Versetzungsdichte und Spannungsfunktionen,” Zeitschrift f�r Phys., vol. 142, no. 4, pp. 463–475, Aug. 1955.

[25] P. Wriggers, Computational Contact Mechanics. Berlin, Heidelberg: Springer Berlin Heidelberg, 2006.

[26] C. Shu and B. E. Richards, “Application of generalized differential quadrature to solve two-dimensional incompressible Navier-Stokes equations,” Int. J. Numer. Methods Fluids, vol. 15, no. 7, pp. 791–798, Oct. 1992.

[27] J. Hirth and J. Lothe, “Theory of Dislocations,” 1982.

[28] C. R. Clayton, “Materials science and engineering: An introduction: by WD Callister Jr.; published by Wiley, Chichester, West Sussex, 1985; 602 pp.; price,£ 40.40.” Elsevier, 1987.

[29] J. W. Kysar, Y. Saito, M. S. Oztop, D. Lee, and W. T. Huh, “Experimental lower bounds on geometrically necessary dislocation density,” Int. J. Plast., vol. 26, no. 8, pp. 1097–1123, Aug. 2010.

[30] G. E. Dieter and D. J. Bacon, Mechanical metallurgy, vol. 3. McGraw-hill New York, 1986.